Monthly Notices
of the
ROYAL ASTRONOMICAL SOCIETY

MNRAS **474,** 886–897 (2018)
Advance Access publication 2017 October 31

doi:10.1093/mnras/stx2815

Planet population synthesis driven by pebble accretion in cluster environments

N. Ndugu,[1]★ B. Bitsch[2]★ and E. Jurua[1]

[1]*Department of Physics, Mbarara University of Science and Technology, P.O. Box 1410, Mbarara, Uganda*
[2]*Lund Observatory, Department of Astronomy and Theoretical Physics, Lund University, SE-22100 Lund, Sweden*

Accepted 2017 October 27. Received 2017 October 25; in original form 2016 December 22

ABSTRACT

The evolution of protoplanetary discs embedded in stellar clusters depends on the age and the stellar density in which they are embedded. Stellar clusters of young age and high stellar surface density destroy protoplanetary discs by external photoevaporation and stellar encounters. Here, we consider the effect of background heating from newly formed stellar clusters on the structure of protoplanetary discs and how it affects the formation of planets in these discs. Our planet formation model is built on the core accretion scenario, where we take the reduction of the core growth time-scale due to pebble accretion into account. We synthesize planet populations that we compare to observations obtained by radial velocity measurements. The giant planets in our simulations migrate over large distances due to the fast type-II migration regime induced by a high disc viscosity ($\alpha = 5.4 \times 10^{-3}$). Cold Jupiters ($r_{\rm p} > 1$ au) originate preferably from the outer disc, due to the large-scale planetary migration, while hot Jupiters ($r_{\rm p} < 0.1$ au) preferably form in the inner disc. We find that the formation of gas giants via pebble accretion is in agreement with the metallicity correlation, meaning that more gas giants are formed at larger metallicity. However, our synthetic population of isolated stars host a significant amount of giant planets even at low metallicity, in contradiction to observations where giant planets are preferably found around high metallicity stars, indicating that pebble accretion is very efficient in the standard pebble accretion framework. On the other hand, discs around stars embedded in cluster environments hardly form any giant planets at low metallicity in agreement with observations, where these changes originate from the increased temperature in the outer parts of the disc, which prolongs the core accretion time-scale of the planet. We therefore conclude that the outer disc structure and the planet's formation location determines the giant planet occurrence rate and the formation efficiency of cold and hot Jupiters.

Key words: accretion, accretion discs – planets and satellites: formation – protoplanetary discs.

1 INTRODUCTION

Most stars are born in stellar clusters (Lada & Lada 2003) and spectroscopic observations have revealed that young stars are rich in circumstellar discs (Lada et al. 2000). The longevity of the protoplanetary disc is a strong function of its environment (Vincke, Breslau & Pfalzner 2015; Vincke & Pfalzner 2016). Discs in stellar clusters face two main hurdles, photoevaporation and stellar encounters that limit both the lifetimes and sizes of discs. Photoevaporation sweeps out materials from the discs rendering shorter lifetimes where the effect is stronger for young stellar clusters (Johnstone, Hollenbach & Bally 1998).

Discs in massive stellar clusters encounter star–disc and disc–disc encounters, which destroy the disc by accreting it on to the central star or capturing part of it by the perturbing star (Steinhausen, Olczak & Pfalzner 2012), making planet formation in young and massive stellar clusters extremely difficult. Nevertheless, Malavolta et al. (2016) observed a multiplanet system in the open stellar cluster M44. Stellar clusters can have hot background temperatures of 40–100 K (Krumholz 2006), which could last during the entire lifetimes of protoplanetary discs until OB stars go supernova. For example, in NGC1333 the highest heating influence of B stars is 40 K (Hatchell et al. 2013). Spaans et al. (1995) also additionally found that young stellar objects can have a heating influence of few hundred Kelvins up to even 1000 au. Embedded discs are thus different from discs of single field stars. The background heating of a protoplanetary discs by a neighbouring star population is attributed to both accretional heating and intrinsic heating of the star population. Here, accretional heating trumpets at the early phase of the star and disc formation process, while intrinsic heating becomes very important within the vicinity of massive stars and at later times.

★ E-mail: ndugu.nelson89@gmail.com (NN); bert@astro.lu.se (BB)

© 2017 The Author(s)
Published by Oxford University Press on behalf of the Royal Astronomical Society

Downloaded from https://academic.oup.com/mnras/article/474/1/886/4582898 by guest on 05 March 2021

Stars in a loosely bound stellar clusters of stellar density less than $\sim$2–3 $\times$ 10^3 pc^{-2} have only a few encounters, like in NGC6791 (Rosotti et al. 2014). This implies that stars in less massive stellar clusters are to a close approximation in an isolated star field but feel the ambient stellar cluster heating. The mentioned stellar density specification for a stellar encounter is well within the definition of stellar cluster in Krumholz (2006). The goal of our work is thus to investigate the influence of a stellar cluster environment on planet formation by focusing on the influence of the stellar cluster on the thermal properties of the disc. We therefore do not model any gravitational encounters between different stars or external photoevaporation, which can significantly alter the disc properties, but rather consider the background temperatures of stellar clusters.

We expand the solar-like disc evolution model of Bitsch et al. (2015a) to mimic the disc evolution model for stellar clusters by setting different background temperatures. In the disc, we implant planetary seeds that have reached the pebble transition mass, indicating that the seeds can accrete in the efficient Hill accretion regime (Lambrechts & Johansen 2014). The planet accretes pebbles rapidly and when it reaches the pebble isolation mass, at which the pebble flux is shut-off due to interactions of the planet with the disc blocking the flux of pebbles, after several 100 kyr (Lambrechts, Johansen & Morbidelli 2014), it contracts an gaseous envelope (Piso & Youdin 2014) and then undergoes run-away gas accretion, when the planetary envelope becomes more massive than the planetary core, where we follow the accretion rates derived by Machida et al. (2010).

Planets migrate through the disc during their entire growth. Small planets that do not perturb the disc significantly, migrate in type-I fashion (Paardekooper, Baruteau & Kley 2011), while massive planets open gaps in the disc and migrate in type-II fashion (Lin & Papaloizou 1986). Our planet growth and migration model is based on the work of Bitsch, Lambrechts & Johansen (2015b), which we expand in order to synthesize planet populations by probing different initial conditions (e.g. metallicity, initial starting semimajor axis of the planetary seeds). The resulting planet populations are then compared with observations to test our predictions, where we focus especially on the metallicity correlation for the formation of giant planets, namely that giant planets form preferably around stars with large metallicity (Fischer & Valenti 2005; Johnson et al. 2010). The metallicity correlation was also studied in planet population synthesis simulations, where the planetary core was growing through the accretion of planetesimals (Ida & Lin, 2004; Matsuo et al. 2007; Mordasini et al. 2009), where the synthetic planet population shows a less steep trend compared to observations.

The work is structured as follows. In Section 2, the different methods used for disc evolution, pebble and gas accretion, and for planet migration and planet population synthesis are described. The disc structure, growth tracks and planet population synthesis simulation and their comparison to observations are presented in Section 3. Then finally, the work is summarized in Section 4.

2 METHODS

2.1 Background heating of stellar clusters

We note here that we do not include the effects of external photoevaporation on to the disc structure, even though external photoevaporation from close by O-stars can significantly change the disc structure and disc lifetime (e.g. Henney et al. 2002), but even within low-mass star-forming regions, external photoevaporation can play a role (Haworth et al. 2017). Here, we investigate instead the change of the temperature field from the background heating of

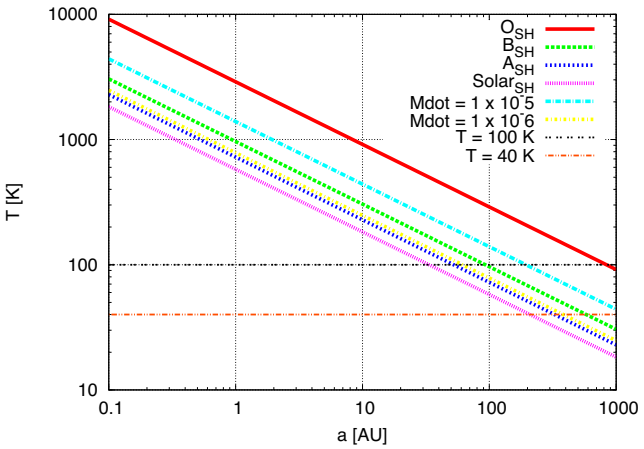


Figure 1. Background heating variation with orbital distance to various heating sources. Protoplanetary discs close to massive stars experience very high background heating. The orange and the black lines display our assumptions of stellar cluster background heating of 40 and 100 K and for which sources this can be maintained. Here, the index SH stands for Stellar heating and $\dot{M}$ represents the accretion rates in Solar mass per year of accreting discs. O, B and A are the spectral classes of stars considered.

stellar clusters, which originates from either accretion luminosity of young stars or from intrinsic stellar luminosity.

During the onset of star formation, the accretion rate on to the new stars is very high, implying very high accretion luminosities, which heat the dust around the central star to very high temperatures. However, as the star ages, the accretion rate reduces by orders of magnitude (Hartmann, Herczeg & Calvet 2016), resulting in reduced accretion rates and accretion luminosities.

Dust around central stars in stellar populations is also heated due to the intrinsic luminosity of massive stars. This heating dominates at late stages of the disc evolution, when accretion is very low. At this stage, heating of a nearby protoplanetary disc is due to the intrinsic luminosity and not through the accretional luminosity. The background heating in a stellar cluster is due to the interplay of accretional and intrinsic luminosity of stars. Accretional luminosity is dependent on the accretion rate while intrinsic luminosity scales with the mass of the stars.

Star populations in a cluster are most often assumed to have the same age. In reality, this is not true because within a stellar cluster, age spreads of stars occur, for example LH 95 hosts an age spread of 2.8–4.4 Myr (Da Rio, Gouliermis & Gennaro 2010). For simplicity of the background heating estimate, we did not consider the age spread of star population in a cluster but assumed a uniform age of star population. Therefore, in our calculation of the ambient stellar cluster heating on to a central star, the adjective 'estimate' is the key.

For a central host star embedded in a population of solar-like stars, the contribution of background heating on to the host star is shown in Fig. 1. Here, we make the simplifying assumption that the heating and cooling of the dust grains happens at the same wavelength, whereas in reality stellar irradiation peaks in the optically, while dust grains emit in the infrared (e.g. Chiang & Goldreich 1997). To obtain Fig. 1, the accretional luminosity is calculated as

$$L_{\rm acc} = \frac{G M_\star \dot{M}_\star}{R_\star} \, . \tag{1}$$

Here ,G marks the gravitational constant, $R_\star$ is the stellar radius, $M_\star$ is the stellar mass and $\dot{M}_\star$ is the accretion rate on to the central star. The intrinsic stellar luminosities were set to the luminosities of

Downloaded from https://academic.oup.com/mnras/article/474/1/886/4582898 by guest on 05 March 2021

O, B, A and solar-like stars. The corresponding luminosities were then translated into a temperature–distance relation displayed in Fig. 1 using the expression

$$\mathrm{T} = \left(\frac{L}{4\pi\sigma R^2} \right)^{\frac{1}{4}} , \tag{2}$$

where L stands for luminosity (intrinsic or accretional luminosity), σ is the Stefan–Boltzmann constant and R is the distance from the star. In Fig. 1, we overplot both the stellar irradiation heating and the accretional heating contribution. It can been seen from Fig. 1 that the influence of accretional heating decreases as the star ages (lower accretional rates) and close massive stars heat the discs to higher temperature. For discs distantly located from the heating stars (1000 au), the background heating of 100 K is not easily achievable from the estimates in Fig. 1.

In stellar clusters with low densities of $\sim$2–3 $\times$ 10^3 pc^{-2}, stars have only few encounters (Rosotti et al. 2014), but the stellar density in these low-density clusters, would be a factor of a few too low to justify background temperatures of 40 K using the temperature estimates of Fig. 1.[1] Nevertheless, Spaans et al. (1995) stressed that heating of a few hundred Kelvins are attainable at 1000 au for stars surrounded by young stellar objects of radiation field of 10 000 K. Background heating of few hundred K were also noticed in Krumholz (2006). From Fig. 1, the background heating of 100 K seems however only to be possible for a location at 100–1000 au from the massive host stars. Therefore, we state here from our rough estimate that the higher background heating of 100 K is only attainable if massive stars are in the cluster, where then external photoevaporation plays a role (Henney et al. 2002). While a background heating of 40 K can even be obtained by intrinsic heating of close massive stars and by the accretion luminosity of young stars. Trailing our background heating calculation, 100 K is an extreme case, implying that the more realistic estimate is 40 K. In the following sections, we apply such background heating of stellar clusters to our disc structure, simulate planet populations using the developed disc structure and test the importance of such discs in mimicking the observed gas giant populations.

2.2 Disc structure and evolution

Protoplanetary discs comprise of dust and gas. Dust particles inside the disc stick and coagulate to form larger pebbles that eventually form planetesimals, for example through the streaming instability (for review, see Johansen et al. 2014). Planetesimals eventually accrete more planetesimals or pebbles to form the even larger planetary cores, which gradually accrete gas when they becomes massive enough. The growth via pebbles and planetesimals depends on the local disc structure, where especially the aspect ratio H/r and the radial pressure gradient play important roles, highlighting the importance of the protoplanetary disc structure for forming planets (Bitsch et al. 2015b; Bitsch & Johansen 2016).

In this study, our disc structure is not a simple power law as in the MMSN (Minimum Mass Solar Nebulae), but is determined by an equilibrium between stellar and viscous heating with radiative cooling. The resulting equilibrium disc structure is determined by the opacity profile of the disc as this determines the cooling rates. Here, our underlying disc model follows Bitsch et al. (2015a).

[1] We have converted the stellar density to a mean star–star distance, giving us estimates about the background temperature using Fig. 1.

The disc dust mass composition is made of the following ingredients; CO (55.9 per cent), CO_2 (9.8 per cent), H_2O (14.3 per cent) and Silicate (20.0 per cent) with evaporation temperatures of 20, 70, 170, 1500 K, respectively, but the disc model only consists of H_2O and Silicate because these are the two species believed to contribute to opacity transitions, in contrast to CO and CO_2, where no transition at the respective ice lines is observed (Qi et al. 2013). The disc's relative abundances follow the findings of Asplund et al. (2009) for solar composition. At the ice line of each ingredient, the fraction of the respective dust ingredient is evaporated, reducing the pebble flux. This implies several ice lines in the disc, where the disc model will take the transitions at the Silicate line and H_2O line into account producing bumps in the disc structure (Bitsch et al. 2015a). The disc structures are not changed at the CO and CO_2 ice lines, as those are only minimal transition of opacity. We used the disc time evolution presented in Hartmann et al. (1998), which is summarized as

$$\log_{10}\left(\frac{\dot{M}_\star}{\mathrm{M}_\odot\ \mathrm{yr}^{-1}} \right) = -8.00 - 1.40 \log_{10}\left(\frac{t + 10^5\,\mathrm{yr}}{10^6\,\mathrm{yr}} \right) . \tag{3}$$

Here, $\mathrm{M}_\odot$ is the solar mass. The stellar accretion rate $\dot{M}_\star$ is related to the viscosity ν and the gas surface density Σ_G as

$$\dot{M}_\star = 3\pi\nu\Sigma_\mathrm{G} . \tag{4}$$

We use here the α viscosity with $\alpha = 0.0054$ as in Bitsch et al. (2015a). We then extend the disc structure calculated in Bitsch et al. (2015a) to mimic the stellar cluster environment. This modification holds for stellar clusters that have few encounters (e.g. NGC6791; Rosotti et al. 2014). Discs in dense stellar clusters experience rampant stellar encounters, which consequently destroys the discs. However, in our model, we did not consider stellar encounters in the cluster, but rather considered a background temperature of 40 or 100 K. The assumption in Krumholz (2006) showed that stellar clusters born from molecular cloud can have background temperature in the range of 40–100 K. The background temperatures hold as long as the stellar cluster is younger than 10 Myr when supernovae clear the remaining gas of the clusters, which interestingly is within the lifetime of protoplanetary discs (Mamajek 2009). Older stellar clusters have lower background temperatures due to fewer remaining stars. The disc model feature $c_\mathrm{s} < v_\mathrm{esc}$, meaning that the disc is bound to the central star, even for large cluster background temperatures.

2.3 Disc profile

Fig. 2 shows the aspect ratio profile for discs in an isolated star field and a clustered star field. The pebble isolation mass (equation 12) and the pebble surface density (equation 8) are directly related to the aspect ratio of protoplanetary discs. Additionally, the migration rates depend on the aspect ratio of the disc, making the aspect ratio profile a strong constraint on planet formation models. From Fig. 2, it can be seen that clustered fields set a high aspect ratio at the outskirts of the disc, compared to isolated field stars. This is due to the stellar cluster dominance over stellar heating of the central star making the outer rim of the disc hotter than for the isolated stars. The hotter outer disc then translates into higher aspect ratios. Additionally, the stellar cluster dominance is pushed to the disc's inner part when the cluster is hotter. The stellar cluster dominance also scales with the accretion rate of the disc. Accretion rates directly relate with the disc's age; young discs have high accretion rates while old discs have low accretion rates. Discs with higher accretion rates are hotter than discs with lower accretion rates due to viscous

Downloaded from https://academic.oup.com/mnras/article/474/1/886/4582898 by guest on 05 March 2021

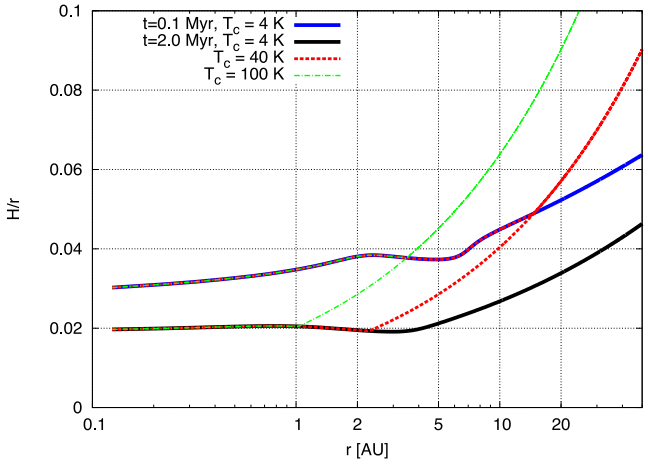


Figure 2. Aspect ratio profile for discs with age $t = 0.1$ Myr (blue) and $t = 2$ Myr (black) around an isolated host star and in stellar clusters with cluster temperatures of 40 K (red) and 100 K (green) for the two ages. In the very inner regions of the disc, viscous heating dominates also over the cluster heating, which is why the disc profiles follow the same trend independent of the background cluster temperature. This is independent of the disc age, but as the disc cools in time, the viscously dominated regions move inwards. For cluster temperatures of 40 K (red) the transition between the viscously dominated part and the cluster heating dominated part of the disc is farther away from the star as for the cluster temperature of 100 K (green).

heating and therefore the influence of stellar clusters on the disc structure increases with time.

2.4 Planet formation and migration model

We grow planets in the core accretion fashion, where pebbles are accreted on to a core, where eventually runaway gas accretion is triggered once the pebble isolation mass is reached and the gaseous envelope contracts. Pebbles with the Stokes number

$$\tau_{\rm f} = \frac{\rho_\bullet R}{\rho_{\rm g} H_{\rm g}}, \tag{5}$$

are accreted on to cores that have reached the pebble transition mass (Lambrechts & Johansen 2012, 2014)

$$M_{\rm t} = \sqrt{\frac{1}{3}\frac{(\eta v_{\rm k})}{G\Omega_{\rm k}}}. \tag{6}$$

Here, $\rho_\bullet$ is the material density, R is the particle radius, $\rho_{\rm g}$ is the gas density, $H_{\rm g}$ is the gas scaleheight, η is the pressure support, G is the gravitational constant, $v_{\rm k}$ is the Keplerian speed and $\Omega_{\rm k}$ is the Keplerian frequency. Initially, the core accretes pebbles in a 3D fashion following the work of Lambrechts & Johansen (2012), because the Hill radius is smaller than the pebble scaleheight for initially low-mass cores. However, as the core attracts more pebbles, it becomes more massive and accretes in a 2D manner because $r_{\rm H} > H_{\rm peb}$ (Morbidelli et al. 2015) with growth rate

$$\dot{M}_{\rm planet} = 2(\tau_{\rm f}/0.1)^{2/3} r_{\rm H} v_{\rm H} \Sigma_{\rm peb}\ , \tag{7}$$

where $r_{\rm H}$ denotes the planetary Hill radius, $v_{\rm H}$ is the Hill speed at which the particles enter (given by $v_{\rm H} = r_{\rm H}\Omega_{\rm K}$) and $\tau_{\rm f}$ is the Stokes number of the pebbles. The pebble surface density is given by

$$\Sigma_{\rm peb} = \sqrt{\frac{2\dot{M}_{\rm peb}\Sigma_{\rm g}}{\sqrt{3}\pi\epsilon_{\rm p} r_{\rm p} v_{\rm k}}}\ , \tag{8}$$

where $r_{\rm p}$ is the orbital distance of the planet. The pebble flux is given by

$$\dot{M}_{\rm peb} = 2\pi r_{\rm g}\frac{{\rm d}r_{\rm g}}{{\rm d}t}\left(Z_{\rm peb}\Sigma_{\rm g}(r_{\rm g})\right.\ , \tag{9}$$

where $Z_{\rm peb}$ is the pebble metallicity, $\Sigma_{\rm g}(r_{\rm g})$ is the gas surface density at the location of the pebble production line $r_{\rm g}$ given by

$$r_{\rm g} = \left(\frac{3}{16}\right)^{\frac{1}{3}} (GM_\star)^{\frac{1}{3}} \left(\epsilon_{\rm D} Z_{\rm peb}\right)^{\frac{2}{3}} t^{\frac{2}{3}} \tag{10}$$

and

$$\frac{{\rm d}r_{\rm g}}{{\rm d}t} = \frac{2}{3}\left(\frac{3}{16}\right)^{\frac{1}{3}} (GM_\star)^{\frac{1}{3}} \left(\epsilon_{\rm D} Z_{\rm peb}\right)^{\frac{2}{3}} t^{-\frac{1}{3}}\ , \tag{11}$$

where $M_\star$ is the stellar mass, $\epsilon_{\rm p}$ and $\epsilon_{\rm D}$ are the pebble and dust coagulation efficiency with values 0.5 and 0.05, respectively. It should be noted that at the ice lines, the pebble flux is significantly reduced by the factor of the corresponding volatile ingredient. Here, we do not take the reduction of the pebble size into account as in Morbidelli et al. (2015), where a reduced pebble size is one of the ingredients to explain the dichotomy between the terrestrial and giant planets of the Solar system. This is the standard pebble accretion paradigm, where $\epsilon_{\rm p}$ and $\epsilon_{\rm D}$ are values corresponding to detailed coagulation simulations, e.g. Birnstiel, Ormel & Dullemond (2011). Within the framework of Lambrechts et al. (2014), the changes of accretion rate could only happen due to changes in coagulation efficiency, which is not motivated by the simulations of grain growth.

We note here that drift limited solution of pebble growth and drift produces pebble surface densities that are a factor of a few lower compared to observations. We therefore incorporate a pebble flux that corresponds to the pebble flux of a protoplanetary disc unperturbed by viscous disc decay outside of 50 au, consistent with viscous disc evolution (Baillié, Charnoz & Pantin 2015). More details of this mechanism can be found in Bitsch, Lambrechts & Johansen (2017).

When the planet reaches a certain mass, it changes the gas pressure outside of its orbit due to a partial opening of a planetary gap, which halts pebble accretion on to the core and gas accretion commences (Lambrechts et al. 2014). The pebble isolation mass is given by Lambrechts et al. (2014)

$$M_{\rm iso} \approx 20\left(\frac{H/r}{0.05}\right) {\rm M_E}\ . \tag{12}$$

This stresses the importance of the disc structure for calculations of planetary growth.

At the pebble isolation mass, the gas envelope contracts over a long time while accreting some gas as long as $M_{\rm env} < M_{\rm core}$ at a rate given by Piso & Youdin (2014) and Bitsch et al. (2015b)

$$\dot{M}_{\rm gas} = 0.002 f^{-2}\left(\frac{\kappa_{\rm env}}{1\,{\rm cm^2\,g^{-1}}}\right)^{-1}\left(\frac{\rho_{\rm C}}{5.5\,{\rm g\,cm^{-3}}}\right)^{-\frac{1}{6}}\left(\frac{M_{\rm c}}{\rm M_E}\right)^{\frac{11}{3}} \times \left(\frac{M_{\rm env}}{0.1{\rm M_E}}\right)^{-1}\left(\frac{T}{81\,{\rm K}}\right)^{-0.5}\frac{\rm M_E}{\rm Myr}, \tag{13}$$

where f is a normalization factor to map the accretion rate on to numerical and analytical results given by 0.2 (Piso & Youdin 2014) and $\kappa_{\rm env} = 0.05\,{\rm cm^2\,g^{-1}}$ is the planet's envelope opacity very similar to the study by Movshovitz & Podolak (2008). $\rho_{\rm C}$ is the core density and we assumed $\rho_{\rm C} = 5.5\,{\rm g\,cm^{-3}}$. The planet continues to contract its envelope until $M_{\rm c} = M_{\rm env}$. When $M_{\rm c} < M_{\rm env}$, rapid gas accretion

Downloaded from https://academic.oup.com/mnras/article/474/1/886/4582898 by guest on 05 March 2021

is triggered and the gas accretion rate is given by the minimum of (Machida et al. 2010)

$$\dot{M}_{\rm gas,low} = 0.83\Omega_{\rm k}\Sigma_{\rm g}H^2\left(\frac{r_{\rm H}}{H}\right)^{\frac{9}{2}} \quad (14)$$

and

$$\dot{M}_{\rm gas,high} = 0.14\Omega_{\rm k}\Sigma_{\rm g}H^2. \quad (15)$$

Low-mass planets migrate in the type-I fashion following the analytical torque formula in Paardekooper et al. (2011), where the total torque, $\Gamma_{\rm tot}$, acting on the planet is given by

$$\Gamma_{\rm tot} = \Gamma_{\rm L} + \Gamma_{\rm C}. \quad (16)$$

$\Gamma_{\rm L}$ and $\Gamma_{\rm C}$ are the Lindblad and corotation torques, respectively. The Lindblad and corotation torques strongly dependent on the local radial gradients of surface density, $\Sigma_{\rm g} \propto r^{-\lambda}$, temperature $T \propto r^{-\beta}$ and entropy $S \propto r^{-\varepsilon}$, with $\varepsilon = \beta + (\gamma - 1.0)\lambda$ and $\gamma = 1.4$ is the adiabatic index. When the planet grows massive enough, it carves gap in the disc (Crida, Morbidelli & Masset 2006) and eventually switches to the slower type-II migration (Baruteau et al. 2014):

$$\tau_{\rm II} = \tau_{\upsilon} \times \max\left(1, \frac{\rm M_p}{4\pi\Sigma_{\rm g}\rm r_p^2}\right). \quad (17)$$

Here, τ_{υ} is accretion time-scale. We combine the disc model, planet formation and migration to synthesize planet populations by sampling the initial conditions. This is described in detail in the following section.

2.5 Initial conditions

Synthesis of a planet population requires a sampling of important input parameters for planet formation. We study the influence of the initial planet starting position, metallicity and disc lifetime. For the disc lifetime and the starting time of the planetary seeds, we assumed a disc lifetime centred around 3 Myr, with a Gaussian distribution with $\sigma = 0.5$ Myr, where we fixed the minimal and maximal lifetime of the disc to 2 and 5 Myr, respectively.

The metallicity of the disc follows a Gaussian distribution centred around 0.0678, where $Z_{\rm tot} = Z_{\rm dust} + Z_{\rm peb} = 1.5$ per cent corresponds to the solar value, [Fe/H]=0. Here, $Z_{\rm dust}$ is the metallicity of the dust grains responsible for the disc structure (Bitsch et al. 2015a), which we set to 20 per cent of the total metallicity $Z_{\rm tot}$. $Z_{\rm peb}$ is the metallicity of pebbles, which corresponds to 80 per cent of the total metallicity $Z_{\rm tot}$. For the initial planetary seed position, we assumed a linear or logarithmic distribution in semimajor axis in the regime of [0.1:50] au.

3 RESULTS AND DISCUSSION

3.1 Growth track

To illustrate the growth mechanism, we use a metallicity of $Z_{\rm peb}$ = 1.2 per cent in pebbles and $Z_{\rm dust}$ = 0.3 per cent in dust for the disc structure, corresponding to [Fe/H] = 0. All planetary seeds in Fig. 3 were implanted at an initial time of $t_0 = 2$ Myr and at different initial positions r_0, implying planets will evolve for 1 Myr, because the disc lifetime is 3 Myr. The starting mass of the planets is different at different positions, because the pebble transition mass is a strong function of H/r and the radial pressure gradient (equation 6). Throughout the study, we used a pebble transition mass obtained for the disc profiles of the isolated field star in order to investigate the different growth mechanisms in detail for the simulations with different cluster temperature. As expected, planetary seeds implanted in clusters with different background temperatures show different growth behaviour, where growth in the outer parts of the disc is significantly reduced in the discs embedded in cluster environments of higher temperature, due to the larger pebble scaleheight allowing only 3D accretion and the loss of volatile pebbles (CO and CO_2).

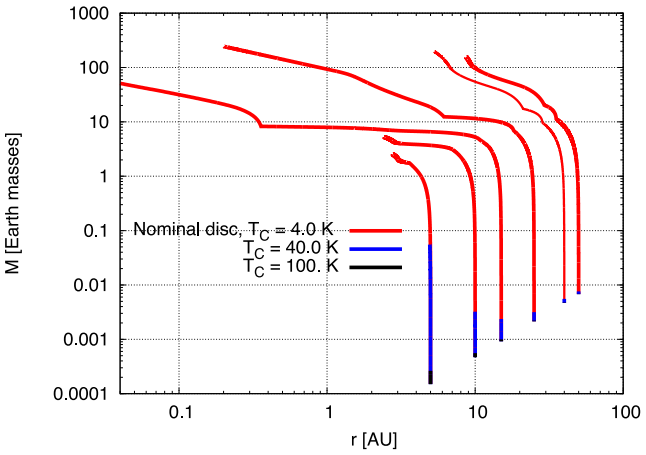


Figure 3. Growth tracks of planets accreting pebbles in an evolving protoplanetary disc submerged in stellar clusters of different heating. Different colours represent the planet's growth in different cluster environments. The planets started growing at 2 Myr up to 3 Myr. In the example of red line, the planet reaches 0.04 au before the disc lifetime and we stopped the simulation. The coloured lines at different r values indicate different types of planet evolution.

Planetary seeds do not grow significantly in disc embedded in clusters with $T > 40$ K. The slow growth rates are a result of the large pebble scaleheight, allowing only 3D pebble accretion in combination with the loss of volatile pebbles that evaporate for these high temperatures (CO and CO_2). Additionally, the growth time is only 1 Myr. In Section 3.2, we vary the lifetime of the protoplanetary disc and the time t_0 at which the planetary seeds are embedded in the protoplanetary disc, which results in further growth. In contrast, the planetary seeds embedded in the disc of an isolated star grow rapidly at all orbital distances, even out to 50 au, because of the smaller pebble scaleheight and the larger pebble flux (all volatile species are available). Note here, that the planet growth rates are higher compared to Bitsch et al. (2015b), because the amount of pebbles $Z_{\rm peb}$ is slightly larger.

In the inner disc ($r < 10$ au), the planets forming in protoplanetary discs heated by cluster environments still do not grow. This is a result of the increased disc scaleheight, the low pebble flux towards the end of the disc's lifetime and the relatively short growth time-scale of 1 Myr. Only in the nominal case, planets can grow. These planets form cores of a few Earth masses that are then parked in the region of outward migration at 2–3 au. They have reached pebble isolation mass and then slowly contract a gaseous envelope. However, the gas contraction time-scale is longer than the here used growth time of 1 Myr.

3.2 Planet population synthesis

Fig. 3 shows the growth tracks of planetary seeds implanted at different positions in the disc, fixed in initial starting time, disc lifetime and metallicity. Extending Fig. 3 in the dimensions of initial starting position, disc lifetime and starting time of the planetary

Downloaded from https://academic.oup.com/mnras/article/474/1/886/4582898 by guest on 05 March 2021

seed as well as metallicity, we synthesize a population of 1350 planets by randomly sampling these quantities. We use here an initial starting time of planetary seeds in the interval [0:1] Myr and disc lifetimes of [2:5] Myr. We use RV (radial velocity) data retrieved from the exoplanet.org data base in order to compare our results with observations first. We only rely on RV data, because our simulations calculate the mass of the planet, not the planetary radius for which a sophisticated chemical evolution model of the planet's interior would be needed. In all our population synthesis plots, planets at the top left in the plot are gas giants observable by the RV detection method as defined in Johnson et al. (2010).

Fig. 4 shows the population of the planets synthesized in an isolated stellar field ($T_c = 4$ K), 40 K stellar cluster and 100 K stellar cluster. Stellar clusters heat up the outer parts of the protoplanetary disc, which sets a higher aspect ratio and consequently a higher pebble scaleheight, pebble isolation mass and lower pebble surface density. Additionally, some volatile species are not present in the form of pebbles anymore, because the temperature is higher than their evaporation temperature (CO and CO_2). Forming planets in a disc with high pebble scaleheight hardly reach the pebble isolation mass, if they grow in the outer parts of the disc, because the planets accrete pebbles in the slower 3D accretion regime due to the increasingly high H_{peb} in the outer disc. This explains the reduced number of giant planets synthesized in a clustered stellar field, reflected in the middle and bottom plots of Fig. 4.

In the top plot of Fig. 4, where planets form in a disc around an isolated host star, gas giants form at all metallicities, while clearly larger metallicities are needed for giant planets forming in discs around stars embedded in clusters. For all these simulations, the final masses of cold Jupiters ($r > 1$ au) can be reproduces quite well, however, the masses of hot Jupiters ($r < 0.1$ au) are overestimated by up to a factor of 10 compared to the RV data. This is related to the fact of the long planetary evolution time compared to the disc lifetime (in contrast to Fig. 3), which allows planets to grow further and become more massive while migrating inwards. The effects of the lifetime of protoplanetary disc on the formation efficiency of giant planets will be discussed in Section 3.3.

Observation of exoplanets have shown that gas giants preferably form at high metallicity, but hardly form at low metallicity (Fischer & Valenti 2005; Johnson et al. 2010). This is contrary to the synthesized planet population in the isolated star fields (the top plot of Fig. 4), where we find in total that 32.2 per cent of our synthesized planets are super-Earths, 8.9 per cent are Neptunian/Saturnian planets, 49.7 per cent are gas giants (hot, warm or cold Jupiters) and 9.2 per cent are low-mass planets (see Table 1). Even though our simulations have a wide spread of metallicity, it implies that these simulations form too many gas giants compared to observations. We will discuss about the metallicity relationship in detail in Section 3.4. In contrast, the amount of small planets increases for planets forming around stars that are embedded in a stellar cluster (see Table 1). Observations of exoplanets have also revealed that nearly 50 per cent of all stars are orbited by rocky planets within 1 au (Mayor et al. 2011), indicating that the isolated field star disc model with a linear starting configuration of planetary seeds is not necessarily likely, as it fails to reproduce the observations.

Because the exact starting position of planetary seeds is unknown at the moment, we expand our study to test the influence of a logarithmic radial starting distribution of the planetary seeds and the results are shown in Fig. 5. The maximum mass a planet can grow to is determined by the disc's aspect ratio, because this sets

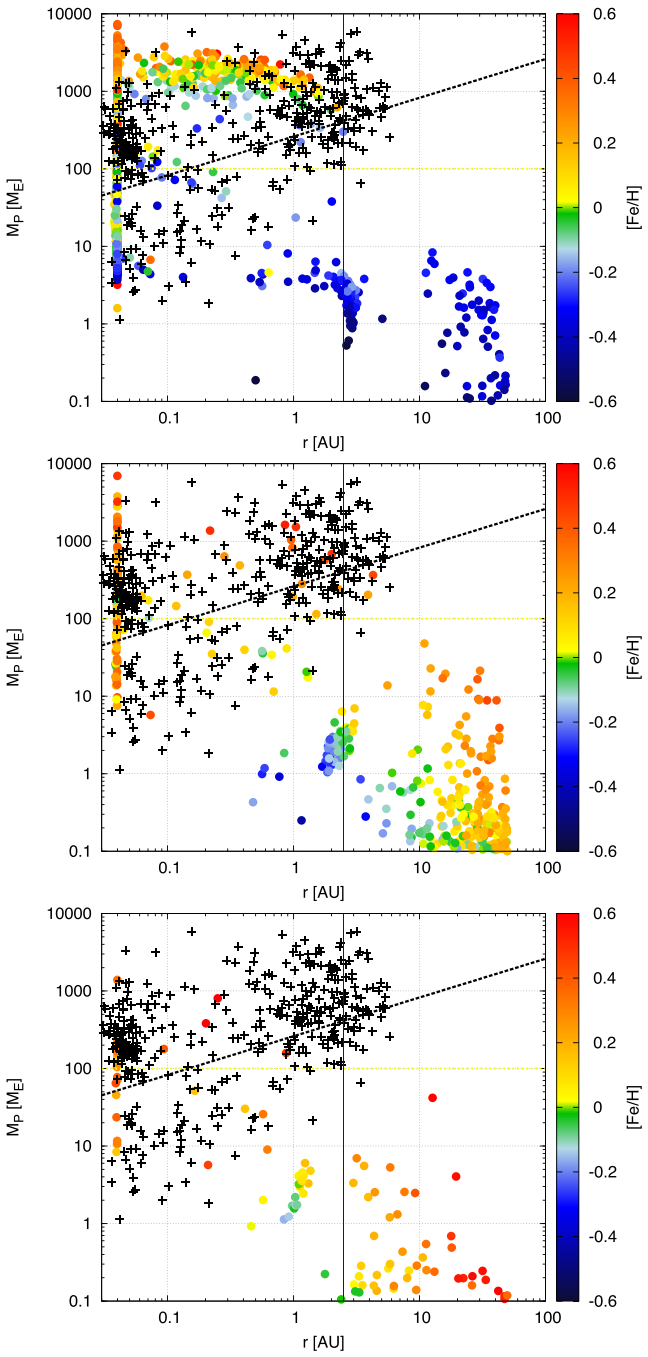


Figure 4. Planet population synthesis for cluster of 4 K (top plot), 40 K (middle plot) and 100 K (bottom plot), respectively, with initial starting time between 0 and 1 Myr and with the linear distribution in starting positions. Different colours features different metallicity values. The disc lifetime spans [2–5] Myr. The black crosses represent RV data retrieved from the exoplanet.org data base. The diagonal black line marks the RV detectability with $K = 20$ m s^{-1}. The vertical blue line marks 2.5 au, which is the radial cut-off for our giant planet frequency calculations and the yellow horizontal line marks 100 Earth masses, which we use as a division between giant planets and no giant planets. Planets inside the top left quadrant represent giant planets that were observed until completeness by the RV survey of (Johnson et al. 2010).

Downloaded from https://academic.oup.com/mnras/article/474/1/886/4582898 by guest on 05 March 2021

Table 1. Proportions of synthesized planets in per cent for the linear starting distribution (top) and for the logarithmic starting configuration (bottom). Here, SE, NP and others depicts super Earth planet ($2M_E < M_P < 16M_E$), Neptunian/Saturnian planet ($16M_E < M_P < 100M_E$) and other planet ($M_P < 2M_E$), respectively. HJ, WJ, and CJ stand for hot Jupiters ($r_p < 0.1$ au), warm Jupiters (0.1 au $< r_p < 1.0$ au) and cold Jupiters ($r_p > 1.0$ au), where all Jupiter-type planets have $M_P > 100M_E$. The population statistics features simulation result for starting time [0:1] Myr and disc lifetime [2:5] Myr, shown in Figs 4 and 5.

		Linear starting configuration:				
$T_c(K)$	SE	NP	HJ	WJ	CJ	Others
4	32.2	8.9	32.4	16.1	1.2	9.2
40	5.3	3.3	10.7	0.7	0.7	79.3
100	1.9	0.6	1.2	0.0	0.0	96.3
		Logarithmic starting configuration				
4	37.2	11.8	35.3	3.6	0.2	11.9
40	24.6	3.9	24.0	0.5	0.0	47.0
100	15.8	1.9	5.3	0.0	0.0	77.0

the pebble isolation mass defining the final mass of the planetary core (equation 12). In the inner parts of the protoplanetary disc, the aspect ratio is smaller (Fig. 2) and thus the pebble isolation mass is smaller. As can be seen from Fig. 3 planetary seeds forming in the inner parts of the disc stay small during their evolution. The logarithmic starting configuration of the planetary seeds therefore results in a much higher super-Earth abundance compared to the linear starting configuration, where more planetary seeds form in the outer parts of the disc. Our findings are that the isolated field star produces a much higher ratio of super Earths, highlighting the importance of the starting position of the planetary seed. Super Earths formation is possible here in contrast to Bitsch et al. (2015b), because of cores forming in the inner disc ($r < 3$ au). Notably, the pile up of planets at 2–3 au disappeared for hotter clusters for the population synthesis simulations with logarithmic distribution (see Fig. 4). This is because hot clusters set higher negative power indices in the surface density gradients which translates into faster inwards migration, destroying the region of outward migration at 2–3 au, which is present for $T_c = 4$ K.

Additionally, the fraction of hot and cold Jupiters ($r_p > 1$ au) is greatly reduced with increasing stellar cluster background temperatures. This is caused by the reduced core accretion rates for planetary cores, forming in the outer disc. However, our simulations still produce a significant fraction of hot-Jupiter-type planets ($r_p < 0.1$ au), because the seeds for most of the hot Jupiter planets form around 5 au, where growth is not reduced as much as compared to even larger orbital distances, where some of the hot Jupiters form that migrate all the way to the central star. On top of that, seeds forming in the outer disc have a harder time opening deep gaps and transition to the slower type-II migration, because of the elevated scaleheight in discs embedded in cluster environments (Fig. 2). The few planetary seeds that grow to Jupiter mass in the outer disc are thus lost to the inner disc, increasing the hot Jupiter abundance and decreasing the cold Jupiter abundance.

3.3 Influence of growth lifetime

The difference between the disc's lifetime and the planetary seed's implantation time sets the growth time of the planet. Planetary seeds implanted early enough in a disc with long lifetime have more time to grow to become massive planets, while cores implanted late in a disc with short lifetimes hardly grow to even an Earth mass in the

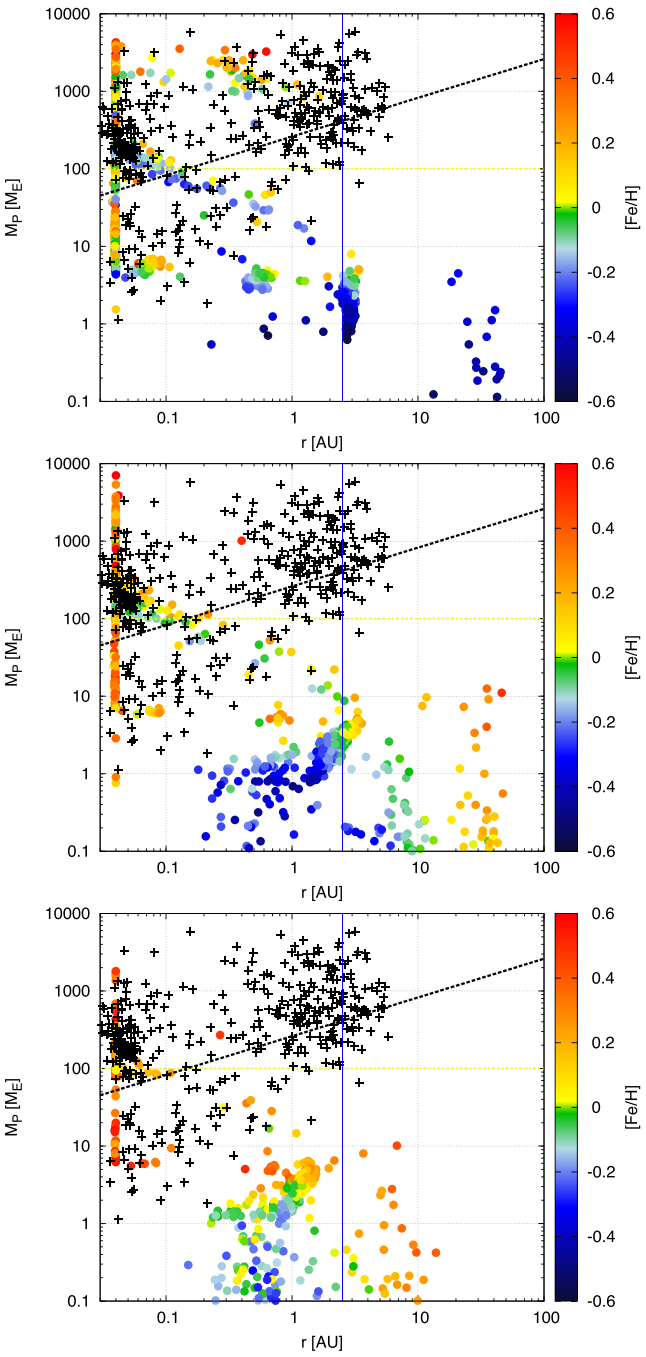


Figure 5. Here, different symbols and colours adopt the same meaning as in Fig. 4. However, it features a logarithmic distribution in the initial planet starting position contrary to linear distribution in Fig. 4.

outer part of the disc, especially if the ambient cluster temperature is high and if the metallicity is low. In principle, a longer disc lifetime could compensate for a lower planetary accretion rate (e.g. due to a lower metallicity), but this also implies that the planet has more time to migrate and this might increase the probability of migrating all the way to the central star. In this section, the effect of the growth time on planet formation is explored.

In Figs 6 and 7, we show the influence of the starting time of the planetary seed on the synthesized planet population. Here, planetary seeds are implanted in a disc that is already [1–2] Myr old, so the planetary seeds have less time to grow compared to Fig. 4. Clearly

Downloaded from https://academic.oup.com/mnras/article/474/1/886/4582898 by guest on 05 March 2021

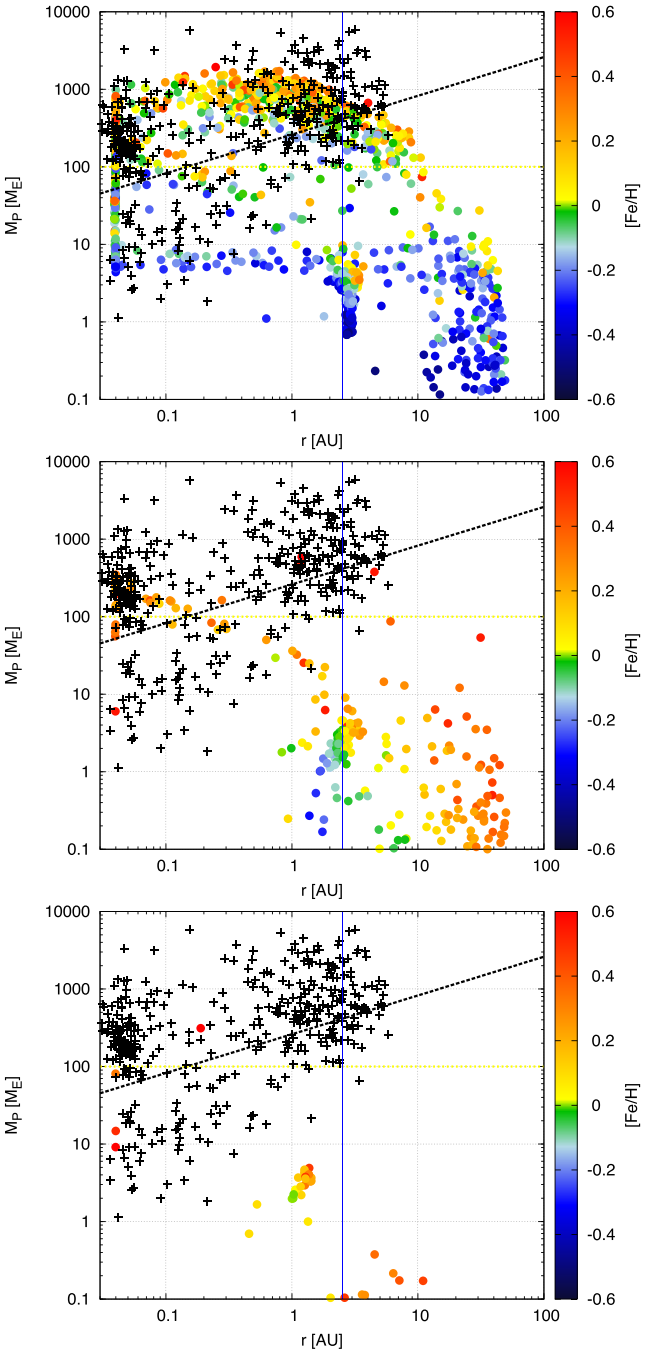


Figure 6. Planet populations synthesized with later starting times of the planetary seeds [1–2] Myr and linear starting positions. Clearly, the planetary masses for the cold and hot gas giants is lower compared to Fig. 4, indicating that the growth time is crucial for the final planetary mass.

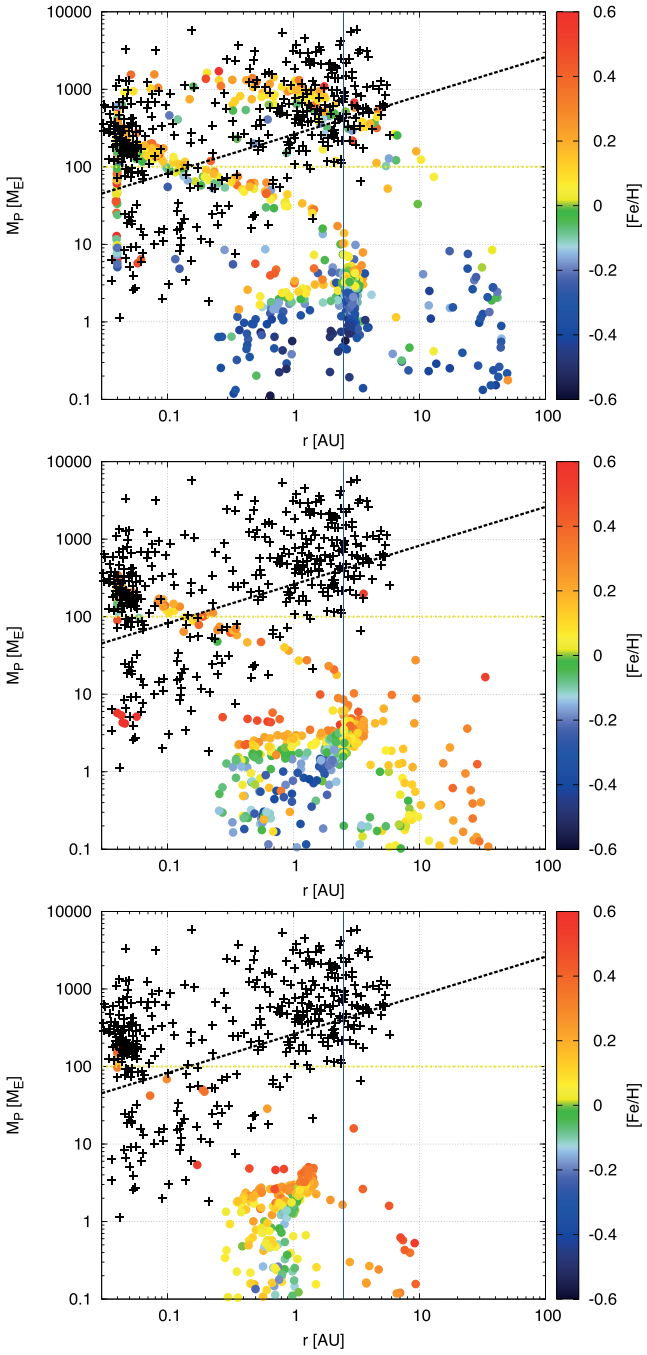


Figure 7. Planet populations synthesized with later starting times of the planetary seeds [1–2] Myr and logarithmic starting positions. The final planetary masses for the cold and hot gas giants is here also lower compared to Fig. 5.

the final masses of the cold Jupiter planets is reduced compared to an early starting time of the planetary seeds. Additionally, the final masses of the hot Jupiter planets is greatly reduced compared to the simulations with early starting time of the planetary seeds. This is of crucial importance, because it allows a much better match to observations, where very massive planets are rarely observed. This hints that a later starting time of the planetary seed might be needed to match observations. Additionally, it could hint at too fast gas accretion rates.

Surprisingly, the fraction of gas giants is similar for the early and late starting times for planets forming in discs without external heating from stellar clusters without external heating from stellar clusters (Table 2). For early starting times, planets forming in the outer disc can grow to Jupiter sizes and have time to migrate all the way to the central star to become hot Jupiters, while later starting times of the planetary seeds result in less growth and also less migration. However, growth is still efficient enough to let seeds formed in the outer parts of the disc grow to become cold Jupiters at a few au. However, both, cold and hot Jupiters are counted as

Downloaded from https://academic.oup.com/mnras/article/474/1/886/4582898 by guest on 05 March 2021

Table 2. Here, the different symbols carry the same meaning as in Table 1 but with population statistics featuring simulation result shown in Figs 6 and 7, where the starting time of the planetary seeds is [1:2] Myr.

$T_c(K)$	SE	NP	HJ	WJ	CJ	Others
Linear starting configuration:						
	SE	NP	GP	Others		
4	25.4	9.8	15.2	16.2	14.8	18.6
40	5.6	1.4	2.6	0.4	0.2	89.8
100	1.2	0.0	0.0	0.0	0.0	98.8
Logarithmic starting configuration:						
4	36.7	6.0	22.2	3.3	4.1	27.7
40	24.2	1.8	5.2	0.5	0.0	68.3
100	9.0	0.4	0.2	0.0	0.0	90.4

gas giants. On the other hand, when planets form in discs exerted to external heating, the giant planet occurrence rate is reduced for later starting times of the planetary seeds. Due to the elevated disc's aspect ratio in the outer disc (caused by the external heating of the disc), the growth time-scale increases. A reduced overall growth time results in less giant planets.

3.4 Metallicity correlation

Observations of giant planets have revealed a strong correlation of giant planets occurrence rate with host star metallicity (Fischer & Valenti 2005; Johnson et al. 2010). In particular, the occurrence rate of giant planets increases with host star metallicity. In the RV observations of Johnson et al. (2010), the giant planet occurrence rate is given by

$$f = 0.07 \times (M_\star/\mathrm{M}_\odot) \times 10^{1.2[\mathrm{Fe/H}]}\,, \tag{18}$$

indicating that 7 per cent of planets orbiting a solar mass star with solar metallicity are giants. Here, we only investigate the planet formation process around solar-type stars. In the sample of Johnson et al. (2010), a giant planet was defined as a planet with velocity semi-amplitudes $K > 20\,\mathrm{m\,s^{-1}}$ within $r < 2.5$ au. This corresponds to a planet of $100\mathrm{M_E}$ at 0.15 au. We now consider from our simulations only planets that have reached the inner disc within 2.5 au with masses $>1\mathrm{M_E}$ and calculate how many of those planets are giant planets ($M_\mathrm{P} > 100\mathrm{M_E}$) compared to small planets as a function of metallicity.[2] The results are shown in Figs 8 and 9 for the linear and logarithmic starting configuration of planetary seeds and for the two different starting times [0–1] and [1–2] Myr, respectively. Additionally, we overplot the giant planet occurrence rate found by Johnson et al. (2010) and shown in equation (18). We have calculated the giant planet fraction in our simulations by taking the ratio between giant planets to small planets within 2.5 au.

Clearly, the efficiency of giant planet formation in the pebble accretion scenario increases with increasing metallicity, for both initial starting configurations. High metallicity allows faster accretion rates (equation 9), which consequently allow cores to reach the pebble isolation mass at an earlier stage, giving more time to contract the gaseous envelope around them and therefore results in an earlier transition to runaway gas accretion, enhancing the formation

[2] We use the $K > 20\,\mathrm{m\,s^{-1}}$ criterion as a limit to define a giant, but with a minimum mass of $100\mathrm{M_E}$.

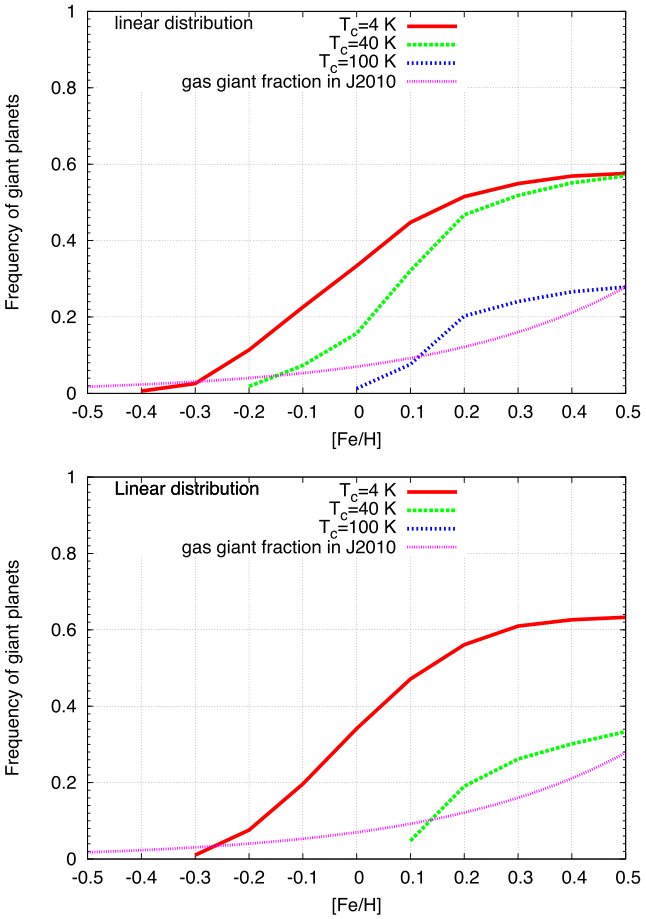


Figure 8. Fractions of host stars harbouring gas giants as a function of metallicity. J2010 stands for Johnson et al. (2010), it reflects the curve in equation (18). For all the clusters, the top plots displays results for starting time [0:1] Myr and the bottom plot shows result for late starting time [1:2] Myr. All the plots feature the linear distribution in the initial starting position of the planetary seeds.

frequency of giant planets. This results in a very efficient pathway to form giant planets.

Giant planet formation is very efficient in the pebble accretion scenario for all cluster temperatures, if the seeds form early. However, the formation frequency of hot Jupiters ($r_\mathrm{p} < 0.1$ au compared to cold Jupiters ($r_\mathrm{p} > 1.0$ au) increases significantly with increasing ambient temperatures of stellar clusters. At late formation times, the picture is similar that hot Jupiters are more common in our simulations compared to cold Jupiters at large ambient cluster temperatures, but at the same time, giant planet formation is greatly inhibited for large ambient cluster temperatures as well (Figs 4–7).

Notably, the starting position of the planetary seeds plays an important role in determining the final mass of the planet, because the pebble isolation mass depends on the position in the disc, where a larger pebble isolation masses can be reached in the outer parts of the protoplanetary disc because of the larger aspect ratio. Planets forming in the outer parts of the disc can thus form cold Jupiters, where their formation is preferred over hot Jupiters at late starting times. Planets forming in the inner disc can only grow to become hot Jupiters because of the rapid inward migration, which prevents planetary seeds to stay at large orbital distances. Therefore, the logarithmic starting configuration results in a lower frequency of cold

Downloaded from https://academic.oup.com/mnras/article/474/1/886/4582898 by guest on 05 March 2021

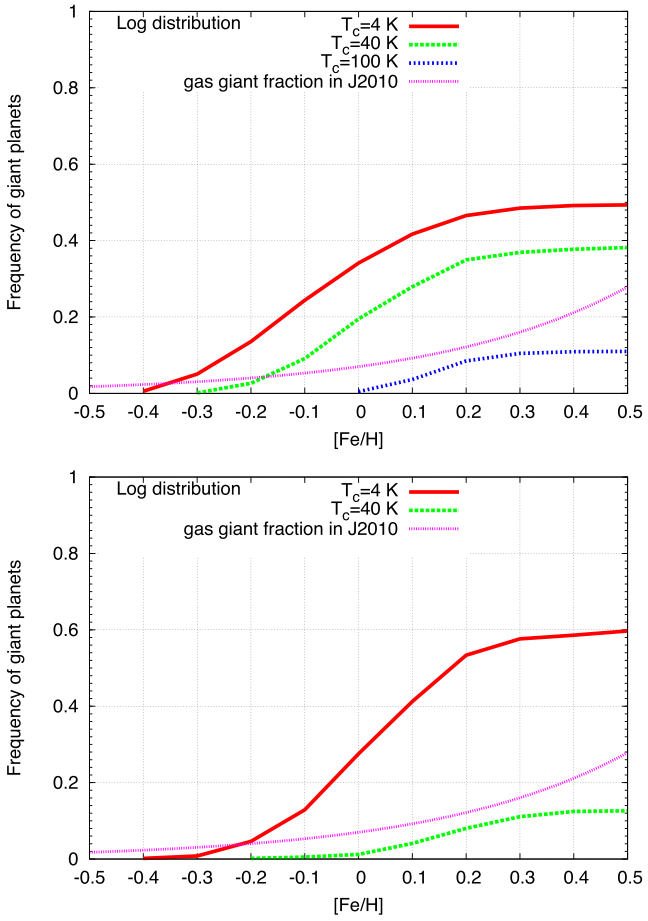


Figure 9. The plots have the same meaning as in Fig. 8 but for a logarithmic distribution in initial starting position.

Jupiters compared to the linear starting configuration of planetary seeds (see Figs 8 and 9).

Our simulations use a one-planet-per-star approach, while most exoplanetary systems host multiple planets. The gravitational interactions between multiple planets can change the formation patterns of planets quite significantly, where an increase of eccentricity reduces the ability to migrate outwards (Bitsch & Kley 2010) and reduces the accretion rate via pebbles (Johansen et al. 2015). In particular, a reduction of the accretion rate might slow down the evolution of planets significantly and thus prevent them to reach the pebble isolation mass, and therefore, they will not accrete a gaseous envelope and not become gas giants. Additionally, if multiple planets are present, scattering events can take place, reducing the number of planets and influencing the statistics (Sotiriadis et al. 2017). We will discuss about different parameters that influence the results of our model in Section 3.5.

In summary, we stress the importance of the following points:

(i) The pebble accretion scenario is in agreement with the metallicity correlation for giant planets, meaning that more giant planets are formed at higher metallicity.

(ii) The initial position of the planetary seeds determines the faith of giant planet formation in our simulations and if a planet can grow to become a gas giant. In particular, a larger aspect ratio in the outer parts of the disc (due to the ambient cluster temperature) reduces the formation efficiency of giant planets, because of the reduced pebble accretion rates. This results in large differences in the metallicity correlation between the planets forming in discs embedded in clusters with different ambient temperatures. Additionally, giant planets formed in discs with large ambient temperatures due to cluster heating form more hot Jupiters than cold Jupiters.

(iii) The initial starting time of the planetary seed influences the growth of the planet itself, as a longer evolution time allows cores to grow to larger planetary masses. It is therefore important when and where a planetary seed forms, which has to be taken into account in future *N*-body simulations that study the evolution and formation of planetary systems.

3.5 Discussion

Our planet formation model is a one-planet-per-star approach, where we probe the formation of giant planets in discs embedded in clusters with different temperatures. The key result of our model is that an increase of the disc's temperature in the outer parts reduces the formation frequency of giant planets and allows in principle a better match to the metallicity correlation of giant planets. However, the cluster temperature also changes the ratio of hot Jupiters compared to cold Jupiters formed in our model. In the following, we discuss about different aspects of our simulations.

(i) In reality, planetary systems consist mostly of multiple planets and not single planets. In our model, we have not taken the effects of multiplicity on the growth of planets into account. Multiplicity is very important, because dynamical interactions of planetary seeds can increase their eccentricity and inclinations, so that the accretion rate as well as the migration rate is greatly reduced (Bitsch & Kley 2010; Levison, Thommes & Duncan 2010). Additionally, many giant planets have a non-zero eccentricity, meaning that scattering with other objects has taken place (Sotiriadis et al. 2017).

(ii) Stellar clusters not only influence protoplanetary discs with ambient background temperatures as in our model but also influence gravitationally. Fly-bys by other stars in the cluster can destroy protoplanetary discs and significantly change the orbits of planets around the central star. These effects could greatly reduce the giant planet occurrence rates. However, our model treats stellar clusters with densities low enough that encounters are not likely (Rosotti et al. 2014). Additionally, the proximity of protoplanetary discs close to O-stars can drive significant external photoevaporation of discs, changing their structure and evolution (Henney et al. 2002). In particular, a shorter evolution time results in a reduced giant planet formation rate in cluster environments.

(iii) When pebbles drift across ice lines in protoplanetary discs, they lose their volatile component. We have taken this effect into account by reducing the pebble flux whenever an ice line is crossed. However, we did not change the size of the pebbles when they crossed the different ice lines. In Morbidelli et al. (2015), this effect was used to explain the great dichotomy between the giant planets and the terrestrial planets, where (as one of the aspects) the larger pebble size at $r > r_{\rm ice}$ allows the outer planetary seeds to grow faster and form the core of gas giants of the Solar system. However, it is yet unclear how much the pebble size should reduce when a specific ice line is crossed. A reduction of the pebble size would thus slow down the accretion rates, especially in discs around stars embedded in clusters where the ambient temperature is higher than the evaporation temperatures of some species.

(iv) Our disc simulations feature only one given α value for the viscosity. A larger viscosity would result in a larger pebble scaleheight, reducing the accretion rate on to the planets and thus lowering the giant planet formation efficiency. A lower viscosity has

Downloaded from https://academic.oup.com/mnras/article/474/1/886/4582898 by guest on 05 March 2021

the opposite effect and reduces the pebble scaleheight and would allow for faster pebble accretion, presumably enhancing the giant planet formation efficiency. Furthermore, the viscosity determines the migration rates, where a higher α-value allows for faster type-II migration and a lower α-value for slower type-II migration.

Our simulations clearly show that cold gas giants form in the outer parts of the protoplanetary disc, while super-Earth-type planets and hot Jupiters form in the inner part of the protoplanetary disc. This has important implications also for the chemical composition of planets, which can be traced in planet formation simulations as well (Madhusudhan et al. 2017) and can be constraint by observations. In particular for gas giants, Madhusudhan et al. (2017) found that there is a distinct difference in the C/O ratio of the planetary atmosphere depending on the formation location if the planet itself. Future additional observations of exoplanetary atmospheres, also of hot super-Earths, can therefore help to constrain planet formation models and can shine light on the question if the seeds of giant planets form only in the outer parts of the disc, as in our model.

4 CONCLUSION

In this study, we combined pebble accretion (Ormel & Klahr 2010; Lambrechts & Johansen 2012, 2014; Lambrechts et al. 2014; Bitsch et al. 2015b; Morbidelli et al. 2015), gas accretion (Machida et al. 2010; Piso & Youdin 2014) and planet migration (Crida et al. 2006; Crida & Morbidelli 2007; Paardekooper et al. 2011; Baruteau et al. 2014) in a disc model, extrapolated from the disc structure of Bitsch et al. (2015a), taking into account the background heating by the stellar cluster. We used this model to synthesize a planet population that allows us to compare our results to observations.

Our planetary seeds start at the pebble transition mass (between 10^{-4} and $10^{-2}M_E$) and grow by subsequent accretion of pebbles. As soon as the planet reached the pebble isolation mass, the flux of pebbles on to the planet is stopped and the gaseous envelope can contract, where the contraction rate is dependent on the mass of the planetary core. In this scenario, larger planetary cores allow for a more rapid envelope contraction, giving more time to the growing planet to reach the runaway gas accretion phase and become a gas-dominated planet. The final core mass depends here on the initial position of the planetary seed, because the pebble isolation mass is a strong function of the disc's aspect ratio. In our case, this means that planets have to reach larger core masses in the outer regions of the protoplanetary disc due to the flaring nature of the disc's structure.

The entire accretion phase occurs concurrently with planet migration. During the initial stage of planet formation, the planet grows by accreting pebbles while exerting negligible perturbation on to the surrounding disc. At this stage, the planet undergoes type-I migration. Planets in the outer disc undergo inward migration due to the shallow radial gradients in temperature, while planets in the inner disc may migrate outwards. However, the region of outward migration evolves in time as the disc sheds materials to the central star (Bitsch et al. 2015a). As the planets grow in time, they may outgrow the region of outward migration and drift inwards, where their migration is stopped at the inner edge of the disc. Planets that reach the runaway gas accretion phase can become massive enough to open deep gaps in the disc, transitioning to the slower type-II migration.

Within stellar clusters, disc sizes are strongly limited by stellar encounters at stellar densities exceeding $\sim$2–3 $\times$ $10^3 pc^{-2}$ (Rosotti et al. 2014). In our case, we limited our model to just including the ambient heating from the cluster with temperatures $T_c \leq 100$ K (Krumholz 2006). According to our background heating estimate, a heating of 100 K is not that easily attainable. However, heating of such magnitudes are seen in Spaans et al. (1995) and Krumholz (2006). Therefore, we state here that the cluster with ambient temperature of 100 K is the extreme case. Our disc model does not account for close stellar fly-bys that can disrupt the disc structure and for external photoevaporation from close by stars.

The seeds of cold gas giants have to form in the outer regions of the protoplanetary disc in our simulations, because a larger aspect ratio is needed to form a big enough core that allows runaway gas accretion. For single field stars, this results in a metallicity correlation for giant planets that is much larger than predicted from observations (Johnson et al. 2010). Additionally, the fraction of small planets is lower than the predictions of observations, where roughly 50 per cent of stars should have planets of super-Earths size (Fressin, Torres & Charbonneau 2013). However, in cluster environments the temperature in the outer parts of the disc can be higher than the evaporation temperatures of some volatiles (e.g. CO), which reduces the amount of material available to form the pebbles needed to form giant planets at those distances. This reduces the accretion rates and results in a smaller giant planet occurrence rate per star for stars embedded in stellar clusters. However, on the other hand this means that as the fraction of giant planets decreases, the fraction of small planets increases, which is more consistent with observations.

Our simulations reproduce the metallicity correlation for giant planets, meaning that more giant planets are formed around stars with larger metallicity. However, in the standard pebble accretion model (Lambrechts & Johansen 2014; Bitsch et al. 2015b), the formation frequency of giant planets is very efficient and might even overpredict the formation efficiency of giant planets. As the pebble accretion rate crucially depends on the disc's aspect ratio, a change of the outer disc structure influences the formation frequency of giant planets. Protoplanetary discs around stars embedded in stellar clusters are subject to the ambient heat from the forming cluster (e.g. Krumholz 2006), which increases the aspect ratio of the outer disc and thus increases the pebble accretion time-scale and therefore reduces the formation frequency of giant planets. However, not all stars remain during their first few Myr in the stellar cluster environment and might leave the cluster and with it the ambient temperature field before their protoplanetary disc dissipates. Therefore, our results reflect a minimum giant planet efficiency for planets formed in a cluster environment with the assumptions that star–star interactions and external photoevaporation play only a minimal role.

Large ambient temperatures allow only for a small fraction of giant planets, unless the metallicity is very large. The formation of super Earths is possible for seeds forming in the inner parts of the disc ($r < 3$ au), where the pebble isolation mass is small, allowing only the formation of cores so small (a few Earth masses) that will not enter into runaway gas accretion during the disc's lifetime. Additionally to that, the disc's metallicity plays an important role, because discs with lower metallicity harbour regions of outward migration in the inner disc that can only contain very low-mass planets (Bitsch et al. 2015a), which allows the inward migration of formed super Earths from beyond the ice line (Bitsch et al. 2015b; Bitsch & Johansen 2016). In our simulations with logarithmic starting configurations, our simulations show a super Earth frequency

Downloaded from https://academic.oup.com/mnras/article/474/1/886/4582898 by guest on 05 March 2021

of about 38 per cent, in rough agreement with observations (Fressin et al. 2013).

In our model, cold Jupiters ($r_p > 1$ au) form preferably in the outer parts of the disc due to the large-scale inward migration. However, their formation is only efficient at low ambient cluster temperatures, and at late formation times of the planetary seeds, implying that maybe standard gas accretion rates are overestimated. Hot Jupiters ($r_p < 0.1$ au), on the contrary, can also form in the outer disc, but then they have to form at early times in discs with long lifetimes to allow efficient migration all the way to the central star. Another formation pathway for hot Jupiters is their initial formation in the inner parts of the disc ($r_{initial} \approx 5$ au), where shorter migration is needed to reach the inner edge of the disc. Additionally, hot Jupiters formed in the inner parts of the disc can also efficiently be formed in discs embedded in clusters with larger ambient temperature. This implies that even with our simple model of cluster environments (ignoring stellar encounters and external photoevaporation), the formation of cold Jupiters is inhibited in cluster environments, while hot Jupiters can form easier. This is at odds with observations, which show a larger frequency of cold Jupiters compared to hot Jupiters, hinting that cold Jupiters do not form in protoplanetary discs embedded in cluster environments. The outer disc structure and the formation location of the planetary seeds is therefore responsible not only for the giant planet occurrence rate but also for the formation efficiency of cold and hot Jupiters. Future studies thus have to constrain the evolution of the outer protoplanetary disc in cluster environments and the formation location of the first planetary seeds.

ACKNOWLEDGEMENTS

We thank the International Science Program (ISP) for their financial support. We also thank Michiel Lambrechts for proof-reading the manuscript. We thank an anonymous referee whose comments helped to improve this manuscript.

REFERENCES

Asplund M., Grevesse N., Sauval A. J., Scott P., 2009, ARA&A, 47, 481
Baillié K., Charnoz S., Pantin E., 2015, A&A, 577, A65
Baruteau C. et al., 2014, in Beuther H., Klessen R. S., Dullemond C. P., Henning T., eds, Protostars and Planets VI. Univ. Arizona Press, Tucson, AZ, p. 667
Birnstiel T., Ormel C. W., Dullemond C. P., 2011, A&A, 525, A11
Bitsch B., Johansen A., 2016, A&A, 590, A101
Bitsch B., Kley W., 2010, A&A, 523, A30
Bitsch B., Johansen A., Lambrechts M., Morbidelli A., 2015a, A&A, 575, A28
Bitsch B., Lambrechts M., Johansen A., 2015b, A&A, 582, A112
Bitsch B., Lambrechts M., Johansen A., 2017, A&A, 607, A67
Chiang E. I., Goldreich P., 1997, ApJ, 490, 368
Crida A., Morbidelli A., 2007, MNRAS, 377, 1324
Crida A., Morbidelli A., Masset F., 2006, Icarus, 181, 587
Da Rio N., Gouliermis D. A., Gennaro M., 2010, ApJ, 723, 166
Fischer D. A., Valenti J., 2005, ApJ, 622, 1102
Fressin F., Torres G., Charbonneau D., Kepler Team, 2013, American Astronomical Society Meeting Abstracts #221, p. 216.03
Hartmann L., Calvet N., Gullbring E., D'Alessio P., 1998, ApJ, 495, 385
Hartmann L., Herczeg G., Calvet N., 2016, ARA&A, 54, 135
Hatchell J. et al., 2013, MNRAS, 429, L10
Haworth T. J., Facchini S., Clarke C. J., Cleeves L. I., 2017, MNRAS, 468, L108
Henney W. J., O'Dell C. R., Meaburn J., Garrington S. T., Lopez J. A., 2002, ApJ, 566, 315
Ida S., Lin D. N. C., 2004, ApJ, 616, 567
Johansen A., Blum J., Tanaka H., Ormel C., Bizzarro M., Rickman H., 2014, in Beuther H., Klessen R. S., Dullemond C. P., Henning T., eds, Protostars and Planets VI. Univ. Arizona Press, Tucson, AZ, p. 547
Johansen A., Mac Low M.-M., Lacerda P., Bizzarro M., 2015, Sci. Adv., 1, 1500109
Johnson J. A., Aller K. M., Howard A. W., Crepp J. R., 2010, PASP, 122, 905
Johnstone D., Hollenbach D., Bally J., 1998, ApJ, 499, 758
Krumholz M. R., 2006, ApJ, 641, L45
Lada C. J., Lada E. A., 2003, ARA&A, 41, 57
Lada C. J., Muench A. A., Haisch J. K. E., Lada E. A., Alves J. F., Tollestrup E. V., Willner S. P., 2000, AJ, 120, 3162
Lambrechts M., Johansen A., 2012, A&A, 544, A32
Lambrechts M., Johansen A., 2014, A&A, 572, A107
Lambrechts M., Johansen A., Morbidelli A., 2014, A&A, 572, A35
Levison H. F., Thommes E., Duncan M. J., 2010, AJ, 139, 1297
Lin D. N. C., Papaloizou J., 1986, ApJ, 307, 395
Machida M. N., Kokubo E., Inutsuka S.-I., Matsumoto T., 2010, MNRAS, 405, 1227
Madhusudhan N., Bitsch B., Johansen A., Eriksson L., 2017, MNRAS, 469, 4102
Malavolta L. et al., 2016, A&A, 588, A118
Mamajek E. E., 2009, in Usuda T., Tamura M., Ishii M., eds, AIP Conf. Proc. Vol. 1158, Exoplanets and Disks: Their Formation and Diversity. Am. Inst. Phys., New York, p. 3
Matsuo T., Shibai H., Ootsubo T., Tamura M., 2007, ApJ, 662, 1282
Mayor M. et al., 2011, eprint (arXiv:1109.2497)
Mordasini C., Alibert Y., Benz W., Naef D., 2009, A&A, 501, 1161
Morbidelli A., Lambrechts M., Jacobson S., Bitsch B., 2015, Icarus, 258, 418
Movshovitz N., Podolak M., 2008, Icarus, 194, 368
Ormel C. W., Klahr H. H., 2010, A&A, 520, A43
Paardekooper S.-J., Baruteau C., Kley W., 2011, MNRAS, 410, 293
Piso A.-M. A., Youdin A. N., 2014, ApJ, 786, 21
Qi C. et al., 2013, Science, 341, 630
Rosotti G. P., Dale J. E., de Juan Ovelar M., Hubber D. A., Kruijssen J. M. D., Ercolano B., Walch S., 2014, MNRAS, 441, 2094
Sotiriadis S., Libert A.-S., Bitsch B., Crida A., 2017, A&A, 598, A70
Spaans M., Hogerheijde M. R., Mundy L. G., van Dishoeck E. F., 1995, ApJ, 455, L167
Steinhausen M., Olczak C., Pfalzner S., 2012, A&A, 538, A10
Vincke K., Pfalzner S., 2016, ApJ, 828, 48
Vincke K., Breslau A., Pfalzner S., 2015, A&A, 577, A115

This paper has been typeset from a TEX/LATEX file prepared by the author.

Downloaded from https://academic.oup.com/mnras/article/474/1/886/4582898 by guest on 05 March 2021